Contents lists available at ScienceDirect

Sensors and Actuators A: Physical

journal homepage: www.elsevier.com/locate/sna

A coupling RF MEMS power sensor based on GaAs MMIC technology

Zhiqiang Zhang, Xiaoping Liao*, Lei Han

Key Laboratory of MEMS of Ministry of Education, Southeast University, Nanjing 210096, China

ARTICLE INFO

Article history:
Received 27 September 2009
Received in revised form 25 January 2010
Accepted 12 March 2010
Available online 18 March 2010

Keywords:
Microwave power measurement
MMIC
RF MEMS
Intermodulation distortion

ABSTRACT

A wideband 8–12 GHz inline RF MEMS power sensor that is based on sensing a certain percentage of the incident microwave power coupled by a MEMS membrane is presented, and the sensor is accomplished with GaAs MMIC technology. In order to improve microwave characteristics and the frequency response of the output at X-band, an impedance matching structure and a capacitance compensating structure are proposed in the paper. The design of the power sensor with the improved structures has resulted in the measured reflection loss of the sensor less than −17 dB, the insertion loss less than 0.8 dB, and the flatness of the frequency response at X-band. A sensitivity of more than 26 μV mW^{-1} and a resolution of 0.316 mW are obtained at 10 GHz under the normal ambient temperature. The experiment demonstrates the immediate effect of the modulation depth under amplitude modulation (AM) signals on the sensitivity of the sensor. In addition, the measured mechanical resonant frequency (f_o) of the MEMS membrane of the sensor is 110 kHz. The measured results show that the intermodulation (IM) power for Δf = 80 kHz, $P_1 = P_2$ = 10 dBm of the signals is less than −52 dBm, and the input third-order intermodulation intercept point (IIP3) is a large value at $\Delta f = f_o$, so the inline RF MEMS power sensor for $\Delta f > f_o$ will not generate significant intermodulation distortion.

1. Introduction

Radio frequency (RF) power sensors play an important role in wireless applications like power monitoring, gain control or circuit protection. Most of modern personal communication and radar systems require that the RF signal is available during power detection. Recently, two kinds of typical inline microwave power sensors based on MEMS technology have been proposed. Dehe et al. [1–3] developed the inline inserted sensors for the measurement of the power dissipated by the intrinsic ohmic losses of the center conductor of a coplanar waveguide (CPW) line, based on Seebeck effect. Fernandez et al. [4–6] and Vaha-Heikkila et al. [7,8] presented the inline capacitive sensors for the measurement of the capacitive change of a moveable membrane suspended above a CPW line where the signal was traveling, based on the capacitive MEMS technology. However, these sensors include many disadvantages such as the trade-off between the microwave performance and the sensitivity, the large variations of the output as a function of the frequency, and the complex process. All these sensors can be embedded into the RF circuits for the purpose of inline power detection, gain control or circuit protection. However, most of these circuits operate at the higher level of the power, so the linearity of the power sensors is a critical parameter to prevent distortions or interchannel interferences.

In our lab, Han et al. [9] presented the inline coupling microwave power sensor that measures a certain percentage of the incident microwave power coupled from the center conductor of a CPW line by a MEMS membrane and then converted to the output thermovoltage based on Seebeck effect. The power sensor consists of a coupling step and a measurement step, which makes it possible to thoroughly solve the trade-off problem that is suffered from the inserted sensors and the capacitive sensors. In order to obtain the excellent microwave performance and the wideband frequency response, Han et al. [10] presented the design and experiment results of the coupling power sensor with the compensating structures by modifying the gap size of the CPW line and adding the metal–insulator–metal (MIM) capacitor. However, due to the compensated capacitance on the order of several fF, directly adding the MIM capacitor is difficult to be fabricated in the process and can result in the deterioration of the microwave performance. On this basis, this paper presents the impedance matching method by modifying the gap size of the CPW line before and after the MEMS membrane, as well as the capacitance compensating method by adding an open-circuital transmission line, in order to further reduce the effect of the MEMS membrane on the microwave performance and obtain the wideband frequency response of the RF MEMS power sensor. The open-circuital transmission line compensating capacitance compared with directly adding a MIM capacitor can be minimally dependent on the process. The power sensor with the improved structures has many advantages such as higher sensitivity, wider frequency response, lower insertion and reflection losses, excellent linearity, and compatibility with GaAs MMIC

* Corresponding author. Tel.: +86 025 83792632x8807; fax: +86 025 83792939.
E-mail address: xpliao@seu.edu.cn (X. Liao).

0924-4247/$ – see front matter © 2010 Elsevier B.V. All rights reserved.
doi:10.1016/j.sna.2010.03.018

technology. And the measured results also show that the modulation depth influences the output of the power sensor directly. Furthermore, this paper presents an experimental study of nonlinear effects generated by the RF MEMS power sensor to prevent interchannel interferences in the following circuit systems. The experiment demonstrates the power sensor will not generate significant intermodulation distortion in some cases. In this paper, the coupling RF MEMS power sensor can be embedded into a microwave receiver, through inline monitoring the microwave power received, and the power value converted to a DC level, then the DC level controlling a controllable attenuator, resulting in avoiding overload and protecting the following low-noise amplifier when receiving too large the microwave signal.

2. Design of the power sensor with the impedance matching and capacitance compensating structures

The coupling RF MEMS power sensor consists of a microwave power coupler and two indirectly thermoelectric microwave power sensors. The microwave coupler that is similar to a capacitive shunt MEMS switch couples a certain percentage of the incident microwave power into two inputs of the thermoelectric power sensors by a suspended MEMS membrane. Then the two indirectly thermoelectric microwave power sensors convert the coupled microwave power into heat and result in the output thermovoltage, respectively, based on Seebeck effect. Fig. 1 shows a schematic view and the lumped equivalent circuit model of the power sensor with the basic structure.

In Fig. 1(b), port 1 and 2 are the input and output ports, and port 3 and 4 are the coupling ports. Z_0 is the characteristic impedance of the CPW line and the matched resistance. C represents the capacitance between the MEMS membrane and the center conductor of the CPW line, which can couple a certain percentage of the incident microwave power. Because the operating frequencies (8–12 GHz) of the sensor in the paper are much smaller than the series resonant frequency of the membrane, the inductance L and the resistance R_s of the MEMS membrane can be neglected, and the capacitance C of the MEMS membrane can be expressed as [11]

$$C = \frac{\varepsilon_0 bw}{g_0 + (t_d/\varepsilon_r)} + C_f \tag{1}$$

where b and g_0 are the width and the initial height of the membrane; w is the width of the center conductor of CPW; t_d is the thickness of the insulation layer; ε_0 and ε_r are the permittivity of free space and the relative permittivity of the insulation layer, respectively; C_f is the fringing field capacitance of the membrane, which is about 20–50% of the total capacitance.

From Ref. [9], it can be known that the coupling power and the application frequencies of the sensor are mainly determined by the capacitance between the MEMS membrane and the center conductor of the CPW line. So a desirable sensitivity and application frequencies can be realized by designing the dimension of the MEMS membrane in the microwave coupler. When the microwave power is transmitted through the MEMS membrane, an electrostatic force is induced on the membrane [12]. It can cause the membrane deflection and lead to the change of the capacitance between the membrane and the center conductor of the CPW line. The effect of the electrostatic force on the MEMS membrane can be obtained as

$$V = (g_0 - z)\sqrt{\frac{2k}{\varepsilon_0 bw} z} \tag{2}$$

where V is the rms voltage amplitude of microwave signals; z is the downward deflection of the membrane; k is the spring constant of the membrane. Assuming no residual stress of the membrane, the spring constant k is expressed as

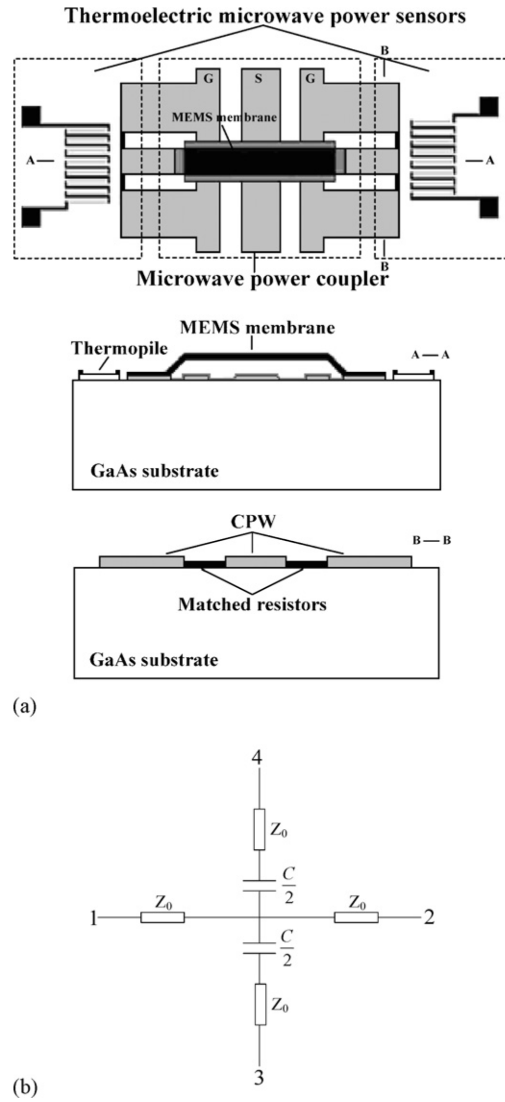

Fig. 1. (a) A schematic view and (b) the lumped equivalent circuit model of the power sensor with the basic structure.

$$k = K\frac{Et^3 b}{l^3} \tag{3}$$

where E is Young's modulus; t and l are the thickness and the length of the membrane; the constant coefficient K is dependent on the location of the evenly distributed force. It can be seen from Eqs. (1)–(3) that varying the width of the membrane can change the capacitance between the membrane and the center line of the CPW but cannot cause the membrane deflection, yet the decrease of the length of the membrane can greatly reduce the deflection at certain rms voltage amplitude. So the width of the membrane will be designed for the realization of the desirable sensitivity, and the length of the membrane will be designed to be very short in order to minimize the effect of microwave signals on the membrane deflection.

In order to reduce the effect of the MEMS membrane on the microwave performance and improve the frequency response of the output thermovoltage, an impedance matching method by modifying the gap size of the CPW line before and after the MEMS membrane, as well as a capacitance compensating method by adding an open-circuital transmission line, is proposed in this paper. Due to the compensating capacitance on the order of several

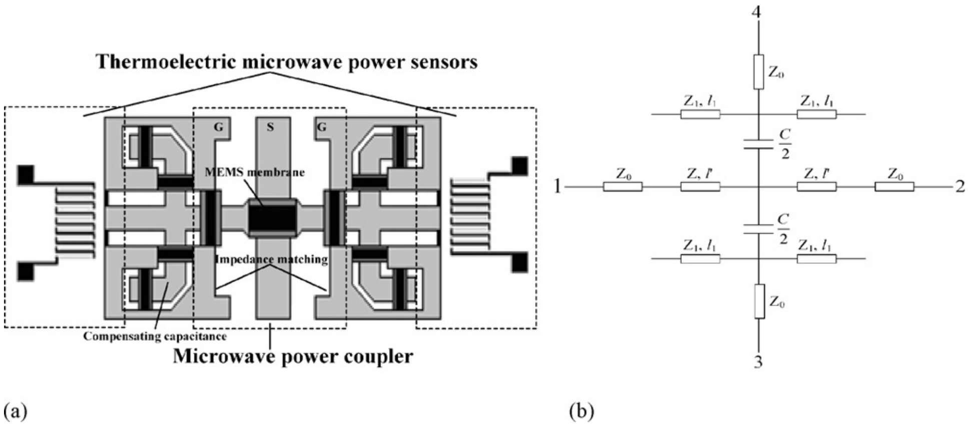

Fig. 2. (a) A schematic view and (b) the lumped equivalent circuit model of the power sensor with the impedance matching and capacitance compensating structures.

fF, directly adding a metal–insulator–metal (MIM) capacitor will strongly depend on the process and cause a significant deviation between the fabricated capacitance and the required capacitance, ultimately result in the deterioration of microwave performance. According to the theory of the transmission line, an open-circuital transmission line can be equivalent to a capacitor. The capacitance compensated by an open-circuital transmission line can be minimally dependent on the process. Fig. 2 shows a schematic view and the lumped equivalent circuit model of the power sensor with the impedance matching and capacitance compensating structures. In Fig. 2(b), Z and l' are the impedance and the length of the uneven CPW line before and after the suspended membrane. Z_1 and l_1 are the impedance and the length of the open-circuital transmission line.

According to the microwave theory, S-parameters of the power sensor with the impedance matching and capacitance compensating structures can be expressed as

the sensitivity of the coupling power sensor in this paper, the GaAs substrate underneath hot junctions of the thermopiles and the matched resistors is removed by hole etching technology, and the thickness of the membrane underneath hot junctions of the thermopiles and the matched resistors is about 10 μm.

3.1. Microwave performance measurement

Microwave performance of the power sensor with the impedance matching and capacitance compensating structures is measured using an Agilent HP8719ES network analyzer and a Cascade Microtech GSG probes station. The measurement of the microwave performance includes the measurement of reflection losses (S_{11}) and insertion losses (S_{21}) of the signal applied to the sensor. Fig. 3 shows a SEM photograph of the power sensor with the impedance matching and capacitance compensating structures.

$$S_{11} = \frac{\begin{array}{l}(j((-2jZ^2(\omega CZ\ \sin^2(\beta l') - \sin(2\beta l')) - \omega CZ^2 Z_0\ \sin(2\beta l') - 2jZ_0^2(\omega CZ\ \cos^2(\beta l') + \sin(2\beta l'))\\ \quad +\omega CZ_0^3\ \sin(2\beta l'))Z_1 + 4Z_0(Z^2(\omega CZ\ \sin^2(\beta l') - \sin(2\beta l')) + Z_0^2(\omega CZ\ \cos^2(\beta l') - \sin(2\beta l')))tan(\beta l_1)))\end{array}}{\begin{array}{l}(2(Z\ \sin(\beta l') - jZ_0\ \cos(\beta l'))(Z_1(Z(-2\ \cos(\beta l') + \omega CZ\ \sin(\beta l')) - 2jZ_0(\omega CZ\ \cos(\beta l') + \sin(\beta l'))\\ \quad +\omega CZ_0^2\ \sin(\beta l')) + 2Z_0(jZ(-2\ \cos(\beta l') + \omega CZ\ \sin(\beta l')) + Z_0(\omega CZ\ \cos(\beta l') + 2\ \sin(\beta l'))tan(\beta l_1)))\end{array}} \tag{4.1}$$

$$S_{21} = \frac{(jZZ_0(Z_1(2 + j\omega CZ_0) + 4jZ_0\ \tan(\beta l_1)))}{\begin{array}{l}((Z\ \sin(\beta l') - jZ_0\ \cos(\beta l'))(Z_1(Z(-2\ \cos(\beta l') + \omega CZ\ \sin(\beta l')) - 2jZ_0(\omega CZ\ \cos(\beta l') + \sin(\beta l'))\\ \quad +\omega CZ_0^2\ \sin(\beta l')) + 2Z_0(jZ(-2\ \cos(\beta l') + \omega CZ\ \sin(\beta l')) + Z_0(\omega CZ\ \cos(\beta l') + 2\ \sin(\beta l'))\tan(\beta l_1)))\end{array}} \tag{4.2}$$

$$S_{31} = S_{41} = -\frac{(4j\omega CZZ_0^2(Z + Z_0)Z_1(-j + \tan(\beta l')))}{\begin{array}{l}(-4jZ^3 Z_1\ \sin(\beta l')\tan(\beta l') + 2Z_0^3(-Z_1(4\omega CZ\ \cos(\beta l') + \sin(\beta l')(2 + 4j\omega CZ + (2j - \omega CZ)\tan(\beta l')))\\ \quad +2Z\sec(\beta l')(-1 + (-3 - 2j\omega CZ)\cos(2\beta l') + 2(-j + \omega CZ)\sin(2\beta l'))\tan(\beta l_1)) + 2Z^2 Z_0(Z_1(2j\ \cos(\beta l')\\ \quad + \sin(\beta l')(-6 - 2j\omega CZ + 3\omega CZ\ \tan(\beta l'))) + 4Z\sin(\beta l')\tan(\beta l')\tan(\beta l_1)) + 2Z_0^4(\omega CZ_1\ \sin(\beta l')(-j + \tan(\beta l'))\\ \quad +4(-j\omega CZ\ \cos(\beta l') + \sin(\beta l')(-j + \omega CZ + \tan(\beta l')))\tan(\beta l_1)) + ZZ_0^2(-\sec(\beta l')(-2j + \omega CZ + (-6j\\ \quad +5\omega CZ)\cos(2\beta l') + (4 + 7j\omega CZ)\sin(2\beta l'))Z_1 + 8Z(-\cos(\beta l') + \sin(\beta l')(-3j + \omega CZ + j\omega CZ\ \tan(\beta l')))\tan(\beta l_1)))\end{array}} \tag{4.3}$$

where $\beta = 2\pi/\lambda$ is the phase shifting constant. And the matched impedance Z through only considering impedance matching conditions can be calculated as

$$Z^3\omega C\ \tan^2(\beta l') - 2Z^2\ \tan(\beta l') + ZZ_0^2\omega C + 2Z_0^2\ \tan(\beta l') = 0 \tag{5}$$

3. Microwave performance measurement and power handling

In this paper, the coupling RF MEMS power sensor is fabricated using GaAs MMIC process with two-layer metal, as described in detail in Refs. [9,10]. The thermopiles are made of gold and n^+ GaAs with a doping concentration of $1.0 \times 10^{18}\ cm^{-3}$. The termination matched resistors (50 Ω) are made of TaN. In order to increase

Fig. 4 shows the measured S-parameters of the sensor with the impedance matching and capacitance compensating structures. In Fig. 4, the measured reflection loss of the sensor is less than −17 dB and the insertion loss is less than 0.8 dB at X-band due to the impedance matching structure. A certain percentage of the total transmitted power is coupled by the MEMS membrane and then converted to the output thermovoltage, so the insertion loss is slightly high. However, the measured reflection and insertion losses are not ideal. It mainly includes the following reasons: the decrease of the fabricated membrane height (g_0) that leads to the increase of the capacitance between the MEMS membrane and the center conductor of the CPW line with the result that much more microwave power is reflected and coupled, and the error of the dimensions of

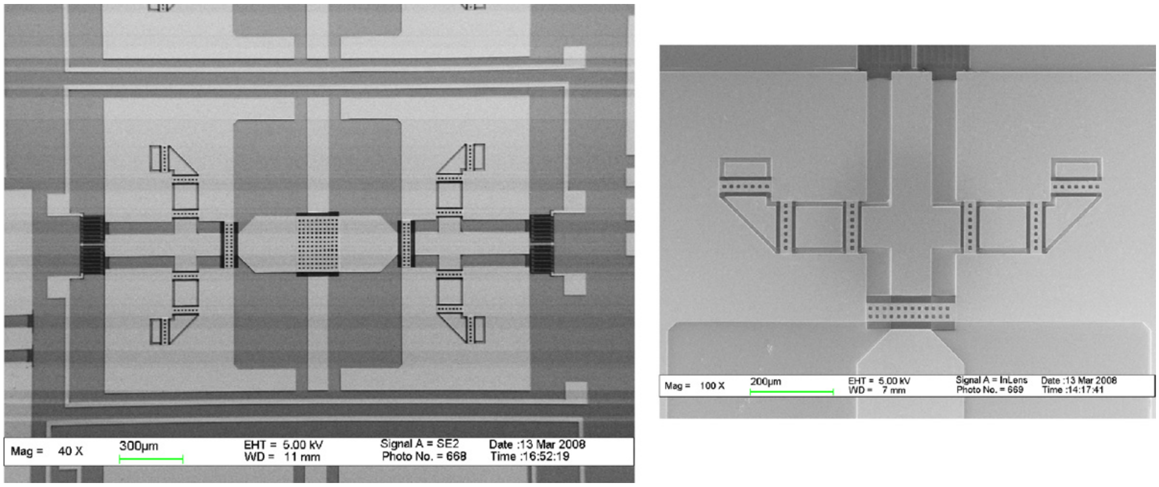

Fig. 3. SEM photographs of (a) the sensor with the impedance matching and capacitance compensating structures and (b) the capacitance compensating structure of the sensor.

the structure in the fabrication that also results in the increase of the reflection and insertion losses.

3.2. Power handling

Power handling of the power sensor with the impedance matching and capacitance compensating structures is measured using an Agilent E8257D PSG analog signal generator, a Cascade Microtech GSG probes station, a 50 Ω loaded resistor, and a Fluke 8808A digital multimeter. The power handling includes the measurements of sensitivities at different frequencies, the frequency response of the output, and the effect of the modulation depths under AM signals on the sensitivities.

Fig. 5 shows the measured output thermovoltage as a function of the microwave power for the power sensor with the impedance matching and capacitance compensating structures under different frequencies. The measurement results demonstrate the excellent linearity of the output thermovoltage with respect to the input microwave power at X-band, and a sensitivity of the power sensor is more than 26 μV mW^{-1} at 10 GHz under the normal ambient temperature. But the sensitivity is slightly decreased because of the open-circuital transmission line dissipating some coupled power. A resolution of the power sensor is on the order of 0.316 mW and is mainly limited by the heat noise of the thermopiles of the power sensor. In Fig. 5, the variations of the output of the power sensor at X-band are small due to the capacitance compensating structure, and it means that the flatness of the output response with respect to the frequency is obtained. Fig. 6 shows the measured output thermovoltage as a function of the frequency for the input power level of 5 dBm. The measured results further show the flatness of the fre-

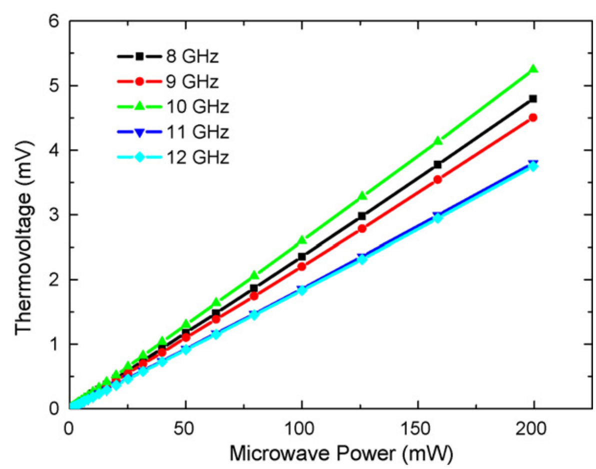

Fig. 5. Measured output thermovoltage as a function of microwave power under different frequencies.

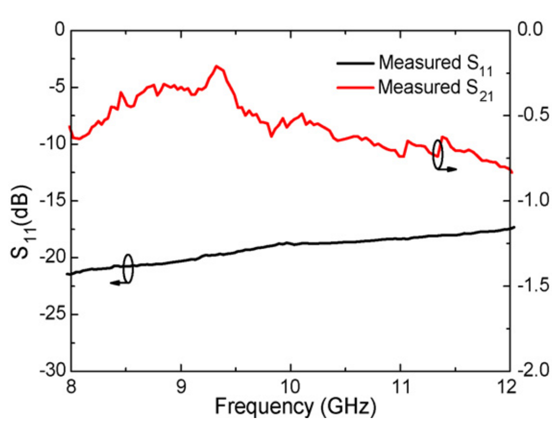

Fig. 4. Measured *S*-parameters of the sensor with the impedance matching and capacitance compensating structures.

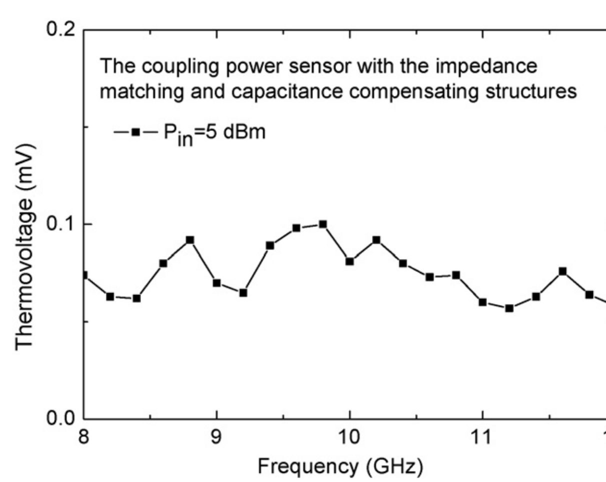

Fig. 6. Measured output thermovoltage as a function of the frequency for the input power level of 5 dBm.

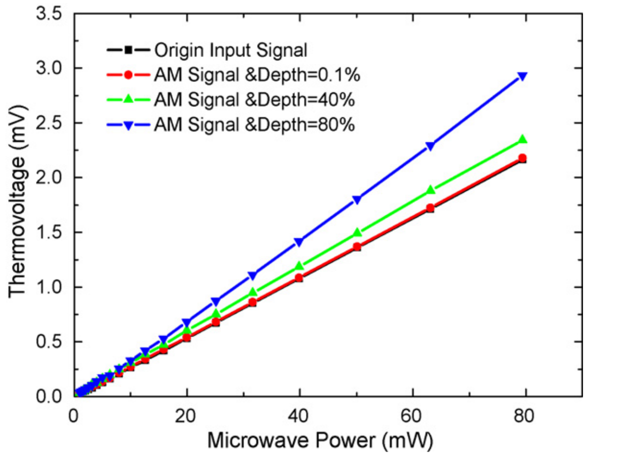

Fig. 7. Measured output thermovoltage as a function of the microwave power under different AM depths at 10 GHz.

quency response at the entire X-band and demonstrate the validity of the capacitance compensating theory.

Fig. 7 shows the measured output thermovoltage as a function of the microwave power for the power sensor with the impedance matching and capacitance compensating structures under different AM depths at 10 GHz. The measurement demonstrates the increase of the output thermovoltage with the modulation depth at 10 GHz when AM signals with the modulated frequency of 10 kHz are applied to the power sensor. The trend is in accordance with that calculated by the AM signal equation in Ref. [12]. Under the AM signals, the sensitivity of the power sensor is almost equal to the origin input signal in the AM depth of 0.1% at 10 GHz, but increases to 30 μV mW^{-1} in the AM depth of 40% and reaches 35.5 μV mW^{-1} in the AM depth of 80%.

4. Intermodulation distortion

Intermodulation distortion of the coupling RF MEMS power sensor with the impedance matching and compensating capacitance structures is measured using two Agilent E8257D PSG analog signal generators, an Agilent E4447A PSA series spectrum analyzer, a Cascade Microtech GSG probes station, and an Agilent 11667C power splitter. Fig. 8 presents the measurement setup of IM distortion. Two RF signals are combined by the −10 dB power splitter. Measurement is done on the wafer and the output spectrum is shown on the spectrum analyzer.

Considering the case of two incident RF signals on the CPW line of the microwave coupler ($V_{in} = V_1 \sin(\omega_1 t) + V_2 \sin(\omega_2 t)$), and assuming $V_1 = V_2$, the IM power at $2f_1 - f_2$ and $2f_2 - f_1$ can be easily calculated as

$$P_{\text{intermod}} = \frac{P_{\text{sideband}}}{P_{\text{signal}}} = \left(V_1 V_2 \frac{\phi C}{4kg_0^2} \right)^2 \qquad (6)$$

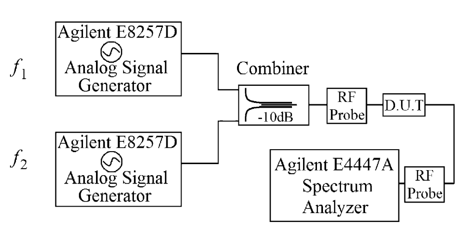

Fig. 8. Measurement setup of IM distortion.

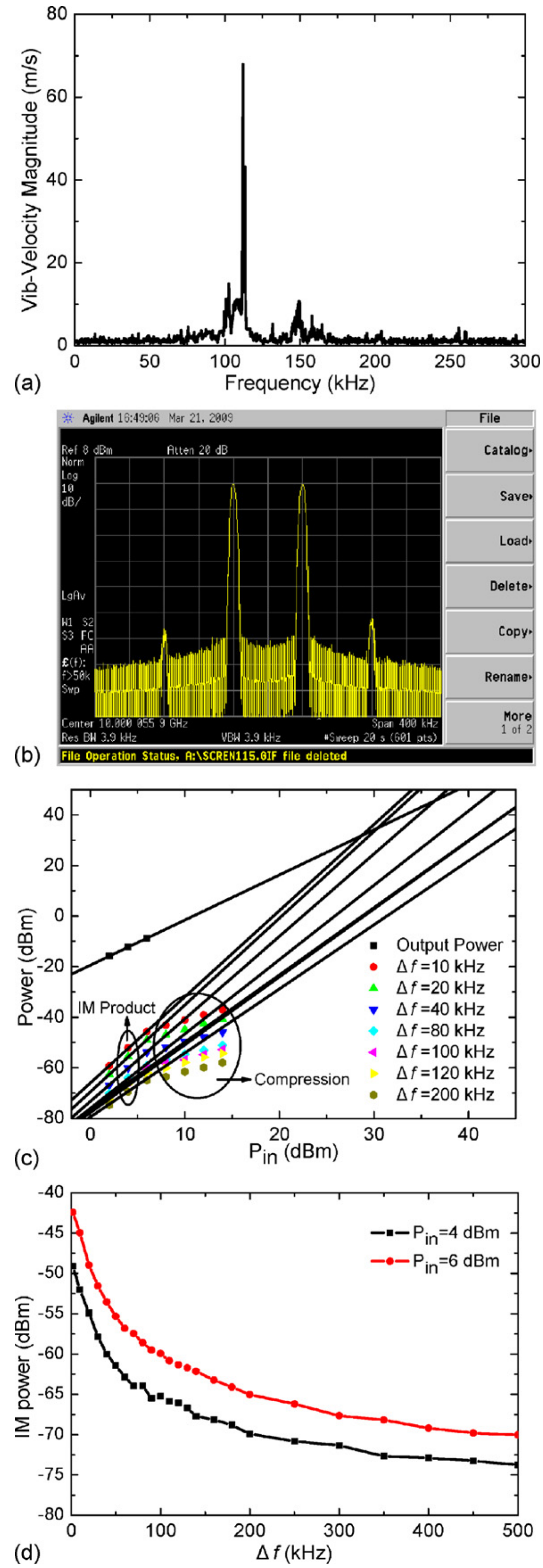

Fig. 9. Measurement of IM products. (a) Mechanical resonant frequency of MEMS membrane. (b) Output spectrum for $P_1 = P_2 = 10$ dBm and $\Delta f = 80$ kHz. (c) Measured results of IM power. (d) IM power versus Δf.

where C is the capacitance of the MEMS membrane; g_0 and k are the initial height and the spring coefficient of the membrane; ϕ is the output phase of the transmission coefficient of the microwave coupler and is given by Rebeiz [12,13]

$$\phi = -\frac{\omega C Z_0}{2} \tag{7}$$

Fig. 9 shows the measurement results of IM products. In Fig. 9(a), the measured mechanical resonant frequency f_o of the MEMS membrane is 110 kHz by the laser doppler vibrometer (LDV), employing the theory of piezoelectric ceramic (PZT) that results in the vibration of the membrane. And the mechanical resonant frequency of the substrate is de-embedded from the measurement results. Fig. 9(b) shows the output spectrum ($\Delta f = |f_2 - f_1| = 80$ kHz, $P_1 = P_2 = 10$ dBm) with an IM product which is lesser than −52 dBm.

The two tone third-order intermodulation intercept point (IIP3) corresponds to the value P_{signal}, where $P_{signal} = P_{intermod}$, and could be easily derived from Eq. (6)

$$\mathrm{IIP3} = \frac{2kg_0^2}{\phi C Z_0} \tag{8}$$

Fig. 9(c) shows the measured results of the IM power. Both the output power and the IM power of the measurement versus the input power could be plotted and the IIP3 could be deduced. From the measurement results, it can be deduced that the IIP3 is +28.7 dBm at $\Delta f = 10$ kHz, but reaches a large value at $\Delta f = f_o = 110$ kHz and it means that the inline RF MEMS power sensor will not generate significant intermodulation distortion.

Fig. 9(d) shows the IM power versus Δf. In Fig. 9(d), IM power remarkably falls off when Δf increases from 2 kHz to 110 kHz, but slightly from 120 kHz to 500 kHz for $P_1 = P_2 = 4$ dBm and 6 dBm. The measurement further demonstrates that the power sensor for $\Delta f > f_o$ will not generate any significant intermodulation distortion in most of the multichannel communication systems.

5. Conclusions

In order to improve microwave characteristics and the frequency response of the output thermovoltage, a wideband 8–12 GHz inline coupling RF MEMS power sensor with the impedance matching and capacitance compensating structures is presented in this paper and the power sensor is accomplished with GaAs MMIC technology. The experiments prove the expected advantages such as higher sensitivity, wider frequency response, lower insertion and reflection losses, and excellent linearity. The modulation depth under AM signals influences the sensitivity of the power sensor directly. Furthermore, the experiment demonstrates that the inline RF MEMS power sensor for $\Delta f > f_o$ will not generate significant intermodulation distortion. The inline wideband RF MEMS power sensor can be widely applied to modern personal communication and radar systems.

Acknowledgments

This work is supported by the National Natural Science Foundation of China (NSFC: 60676043 and 60976094) and the National High Technology Research and Development Program of China (863 Program, 2007AA04Z328).

References

[1] A. Dehe, V. Krozer, K. Fricke, H. Klingbeil, K. Beilenhoff, H.L. Hartnagel, Integrated microwave power sensor, Electron. Lett. 31 (1995) 2187–2188.
[2] A. Dehe, K. Fricke-Neuderth, V. Krozer, Broadband thermoelectric microwave power sensors using GaAs foundry process, in: IEEE MTT-S International Microwave Symposium Digest, Seattle, WA, United states, 2–7 June, 2002, pp. 1829–1832.
[3] A. Dehe, H. Klingbeil, V. Krozer, K. Fricke, K. Beilenhoff, H.L. Hartnagel, GaAs monolithic integrated microwave power sensor in coplanar waveguide technology, in: Proceedings of the 1996 IEEE Microwave and Millimeter-Wave Monolithic Circuits Symposium, San Francisco, CA, USA, 16–19 June, 1996, pp. 161–164.
[4] L.J. Fernandez, J. Sese, J. Flokstra, R. Wiegerink, Capacitive MEMS application for high frequency power sensor, in: Proc. Micromechanics Europe, Rumania, 6–8 October, 2002, pp. 252–255.
[5] L.J. Fernandez, E. Visser, J. Sese, R. Wiegerink, J. Flokstra, H. Jansen, M. Elwenspoek, Radio frequency power sensor based on MEMS technology, in: Proc. IEEE Sens. Conf., Toronto, Canada, 22–24 October, 2003, pp. 549–552.
[6] L.J. Fernandez, R.J. Wiegerink, J. Flokstra, J. Sese, H.V. Jansen, M. Elwenspoek, A capacitive RF power sensor based on MEMS technology, J. Micromech. Microeng. 16 (2006) 1099–1107.
[7] T. Vaha-Heikkila, J. Kyynarainen, A. Oja, J. Varis, H. Seppa, Capacitive MEMS power sensor, in: Proc. 3rd Workshop on MEMS for Millimeterwave Communications, Greece, 2002, pp. 336–339.
[8] T. Vaha-Heikkila, J. Kyynarainen, J. Dekker, P. Pekko, N. Guillaume, A. Oja, J. Varis, H. Seppa, Capacitive RF MEMS power sensors, in: Proc. 3rd ESA Workshop on Millimeter Wave Technology and Application: Circuits, System, and Measurement Techniques, Finland, 2003, pp. 503–508.
[9] L. Han, Q.A. Huang, X.P. Liao, A microwave power sensor based on GaAs MMIC technology, J. Micromech. Microeng. 17 (2007) 2132–2137.
[10] L. Han, Q.A. Huang, X.P. Liao, S. Su, A micromachined inline-type wideband microwave power sensor based on GaAs MMIC technology, J. Microelectromech. Syst. 18 (2009) 705–714.
[11] J.B. Muldavin, G.M. Rebeiz, High-isolation CPW MEMS shunt switches. Part 1. Modeling, IEEE Trans. Microwave Theory Tech. 48 (2000) 1045–1052.
[12] G.M. Rebeiz, RF MEMS Theory, Design, and Technology, Wiley, Hoboken, NJ, 2003.
[13] L. Dussopt, G.M. Rebeiz, Intermodulation distortion and power handling in RF MEMS switches, varactors and tunable filters, IEEE Trans. Microwave Theory Tech. 51 (2003) 1247–1256.

Biographies

Zhiqiang Zhang was born in China in 1983. He received the B.S. degree in 2006 from Hefei University of Technology, Hefei, China. He was admitted in 2007 for the M.S. degree by the Key Laboratory of MEMS of Ministry of Education, Southeast University, Nanjing, China, and then became a Ph.D. candidate in 2009. Now he is currently working toward the Ph.D. degree in the Key Laboratory of MEMS of Ministry of Education, Southeast University. His current research interests include RF MEMS power sensors and passive filters.

Xiaoping Liao was born in China in 1966. He received the B.S. and Ph.D. degrees in electronic engineering from Southeast University, Nanjing, China, in 1987 and 1998, respectively. He was a postdoctoral researcher at Hong Kong University of Science and Technology, Kowloon, Hong Kong, in 2002, where his research involved RF SOI power MOSFETs. He is currently a full Professor at the Key Laboratory of MEMS of Ministry of Education, Southeast University. He focuses on RF MEMS devices and circuits, particularly on RF MEMS switches and microwave power sensors.

Lei Han was born in China in 1982. He received the B.S. degree in 2003 from Hefei University of Technology, Hefei, China, and the M.S. degree in 2006 from Southeast University, Nanjing, China, where he is currently working toward the Ph.D. degree, with interests in design and fabrication of micromachined RF/MW devices on GaAs substrate.